



SYNTHESIS OF METAL ORGANIC FRAMEWORKS (MOF-199) AND IT'S APPLICATION FOR CHROMIUM (VI) ADSORPTION FROM AQUEOUS SOLUTION BY EXPERIMENTAL DESIGN APPROACH

*M. S. Sulaiman^{1, 2}, O. A. Ajayi² and M. S. Olakunle²

¹Department of Pure and Industrial Chemistry, Bayero University Kano, Kano, Nigeria

²Department of Chemical Engineering, Ahmadu Bello University Zaria, Kaduna, Nigeria.

*E-mail of Corresponding author: sdanguguwa@gmail.com

ABSTRACT

The presence of heavy metals in streams arising from the discharge of industrial effluents into water bodies is one of the most important environmental issues because of their toxic nature. Chromium is one of the most widely utilized metals in today's world, making it the most common longstanding environmental contaminant in natural water bodies. In the present study, response surface methodological optimization strategy using central composite design was used for the adsorption of Cr (VI) using metal organic framework (MOF-199) as adsorbent. Effect of various operating parameters such as initial metal concentration, adsorbent dosage and contact time was studied and optimized. From the statistical analysis of the experimental data, the optimum conditions for the maximum removal of metal ions was achieved at a concentration of 10 mg/L, adsorbent dosage of 10 mg and a contact time of 120 minutes. At these optimized conditions, the maximum percentage of Cr (VI) removal was found to be 84%. The adsorbent (MOF-199) was synthesized and characterized using PXRD, FTIR, BET, SEM/EDX and the amount of Cr (VI) adsorbed was measured using UV- spectrophotometer. Adsorption was fit to Langmuir model, the kinetics by pseudo-second order. Gibbs free energy (ΔG°) at standard conditions shows that adsorption processes studied are spontaneous.

Keywords: Adsorption, Central composite design, Chromium (VI), Metal organic frameworks, Heavy Metals.

INTRODUCTION

Due to its serious health problem, Chromium (VI) is considered to be one of the most toxic metals discharged into the environment, mainly by industrial activities (Chagas *et al.*, 2019). Chromium (VI) can be removed from aqueous waste by a variety of techniques, such as chemical reduction followed by precipitation, ion exchange, reverse osmosis and adsorption. Metal organic frameworks (MOFs) materials especially MOF-199 (First synthesized at Hong Kong University of Science and Technology) is one of the most studied as it has large surface area (Mahadi *et al.*, 2015), and has shown excellent adsorption performance (Shi *et al.*, 2017). First reported in 1999 by Chui *et al.*, MOF-199 material is water stable and contains Cu²⁺ dimer as the metallic units linked to oxygen atoms from benzenetricarboxylate ions (Petit *et al.*, 2011). The synthesis of MOF-199 is simple, employs commercial reagents and has been widely investigated under different experimental conditions; recently it has been identified as one

of the most porous MOF (Rodriguez *et al.*, 2015) and among the first MOFs that are commercially available. As in the case of most MOFs, MOF-199 was utilized for several applications. For example, in comparison between MOF-199 and ZIF-8 for the adsorption of phenol(Ph) and p-nitro phenol(PNP), MOF-199 shows higher adsorption capacity of 79.55% for Ph and 89.3% for PNP as compared to 65.5% Ph and 77.0% PNP using ZIF-8 as studied by Giraldo *et al.*, (2017). In another study by Ghorbani-Kalhor (2016), the preparation of a magnetic metal organic framework of type MOF-199 containing magnetite (Fe₃O₄) nanoparticles has shown to represent a viable sorbent for separation and pre-concentration of Cd (II), Pb (II), and Ni (II) ions.

The main goal of this research is to synthesize, characterize and investigate the use of Metal organic frameworks (MOF-199) as an adsorbent for the removal of Chromium (IV) ions from aqueous solution by optimization using the central composite design (CCD).

MATERIALS AND METHODS

General

All chemicals used in this study were of analytical grade. Potassium dichromate (K₂Cr₂O₇) was used as the source of chromium stock solution. Spectroscopic analyses were carried out using a Fourier transform infrared (FTIR) (Perkin-Elmer Spectrum One FT-IR-60036). The surface morphology was visualized by a scanning electron microscope (SEM) coupled with EDX (Zeiss (LEO) 1450VP). Surface area and pore diameter was determined using a gas adsorption surface analyser (BellPrev Vac II, Belsorp max instrument). Also the crystal structure of MOF-199 was determine using X-ray powder diffraction (Bruker D8 ADVANCE diffracto-meter).

Preparation of MOF-199

MOF-199 was synthesized via modified procedure reported by shi *et al.*, (2017). Thus, 2g of Cu(NO₃)₂·3H₂O was dissolved in 25mL of deionized water and 1g of 1,3,5-benzenetricarboxylic acid (BTC) dissolved in a

mixture of 20mL of ethanol with 20mL of DMF and then heated at 140 °C for 24 hours.

Batch Adsorption Experiment

In the current study, experiments were designed via Response surface methodology (RSM). Three (3) parameters were studied using central composite design (CCD) model with the help of design expert software Version 11.0. The range of selected independent variables is presented in Table 1 below. Batch adsorption experiments were conducted to obtain rate and equilibrium data. Each experiment was carried out in 50mL of the chromium solution at an agitation speed of 125 rpm for 120 minutes to reach equilibrium. The adsorbent was separated from the solution using a whatman filter paper, and the separated solution was analysed for residual chromium ion concentration using UV- spectrophotometer. The percentage removal was analyzed using equation (1) below.

$$Uptake(\%) = \frac{C_i - C_f}{C_i} \times 100 \dots\dots\dots 1$$

Where *C_i* = Initial chromium ion concentration, *C_f* = Final chromium ion concentration

Table 1: Experimental range and levels of parameters for Chromium (VI) adsorption

Factors	Coded	Low value	High value
Concentration (mg/L)	A	10	50
Dosage (mg)	B	10	50
Contact Time (Minutes.)	D	15	120

RESULTS AND DISCUSSION

XRD Characterization of MOF-199.

The PXRD patterns of the synthesized MOF-199 (Figure 1) was found to be in agreement with earlier data reported in the literature and also identical with the simulated (according to *Cambridge Crystallographic Data Center*) MOF-

199 (Zhang *et al.*, 2013).This proves the synthetic procedure of MOF-199 (Petit *et al.*, 2011) as well as the crystallized structure of the product (Li *et al.*, 2013; Zhao *et al.*, 2014). The main peaks appeared at 2θ of 6.7°, 9.5°, 11.6°, 13.4°, 17.5° and 19.12°.

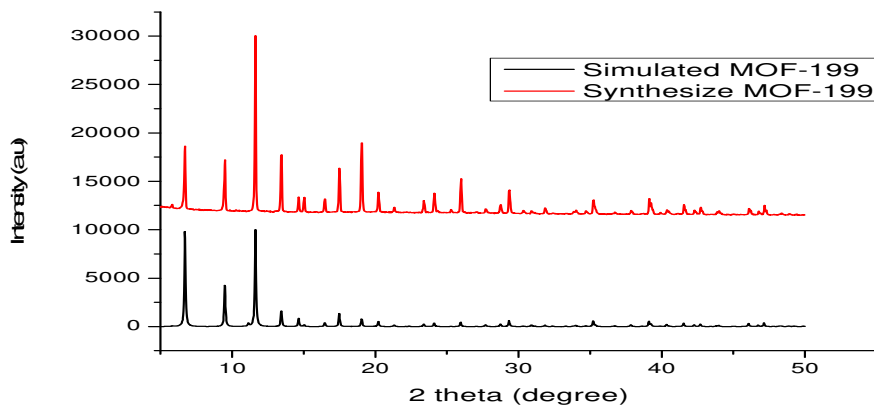


Figure 1 PXRD pattern of MOF-199

FTIR spectra of MOF-199 before and after Cr (VI) Adsorption

The vibrations bands obtained for MOF-199 as shown in Figure 2 shows good agreement with those found in the literature. The absence of peaks between 1720 – 1680 cm^{-1} indicates that deprotonation has taken place (Maleki *et al.*, 2015). The existence of complexation of –COOH groups in the ligand (1,3,5, benzene tricarboxylic acid) with the metal ions can be assigned to the band at 1648 cm^{-1} . This unambiguously indicated that the carboxylate ions participated in the complex formation. The peak at 1448 cm^{-1} comes from the unsaturated Cu^{2+} ion metal centres due to the existence of Lewis acid site on the samples (Shi *et al.*, 2017). The

characteristic vibration at 723 cm^{-1} might be attributed to Cu–O stretching vibration, in which the oxygen atom was coordinated with Cu. Absorption peaks at 490, 598 and 662 cm^{-1} indicates that MOF-199 is free of CuO and Cu_2O during formation of the product (Lestari *et al.*, 2016). The bands at 1648, 1448 and 1112 cm^{-1} corresponded to the asymmetric and symmetric stretching vibrations of the carboxylate groups in benzenetricarboxylic (BTC), respectively (Liu *et al.*, 2020). After Cr (VI) adsorption, the peak at 1648 cm^{-1} shifted to 1614. It was also discovered that the peak at 1109 cm^{-1} has disappeared after the adsorption. The peak values at other sites also decreased, indicating that the addition of Cr after adsorption reduced the strong interaction.

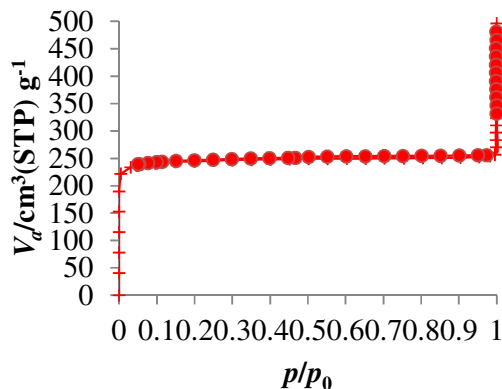
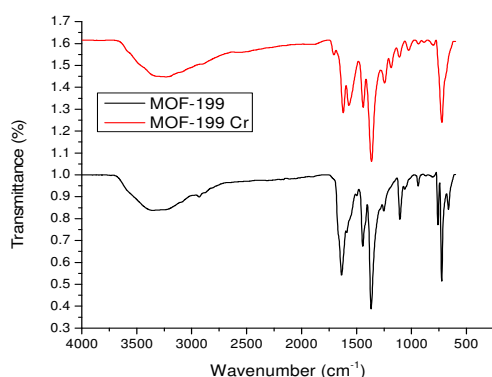


Figure 2 FTIR spectra of synthesized MOF-199 before and after Cr (IV) adsorption.

Figure 3 Nitrogen Adsorption-Desorption Isotherm at 77K for MOF-199

BET Surface Areas and Pore Structure Analysis

The isotherm model of MOF-199 exhibited Type I isotherm (Mahadi *et al.*, 2015) as shown in figure 3 and in accordance with the IUPAC classification with a hysteresis loop that rises sharply at low relative pressure before reaching plateau. This is typical for materials that are microporous and uniform pore distribution (Petit *et al.*, 2011). However, a small hysteresis

accounts for the presence of some mesopores as studied by Alfe *et al.* (2014). In this work, MOF-199 has a BET surface area of 794.07 m^2g^{-1} , (as shown in figure 3) which is in the range of those found in literature (Petit *et al.*, 2011; Zhao *et al.*, 2014; Petit and Bandoz, 2012). Generally, the specific surface area of the synthesized MOF-199 is usually around 700–800 m^2g^{-1} (Liu *et al.*, 2020).

SEM/EDX Topography

Figure 4 shows the SEM, and EDX images of the synthesized MOF-199. MOF-199 sample exhibited an octahedral with a smooth surface (Maleki *et al.*, 2015) and almost no particle agglomeration with a homogeneous particle size distribution (Sheno *et al.*, 2014). This ensures high crystalline and morphological quality of

MOF-199 sample. Furthermore, EDX analysis shows the existence of Copper and Oxygen elements that confirms formation of MOF-199. Moreover, after Cr (VI) adsorption, as shown in figure 5, elemental mapping analysis (EDX) clearly shows that Chromium (VI) was adsorbed on the the surface of MOF-199.

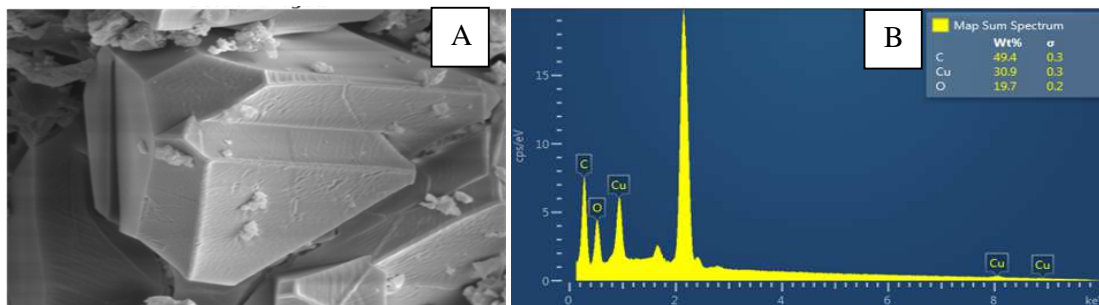


Figure 4. SEM (A) and EDX (B) of MOF-199 before Cr (VI) adsorption.

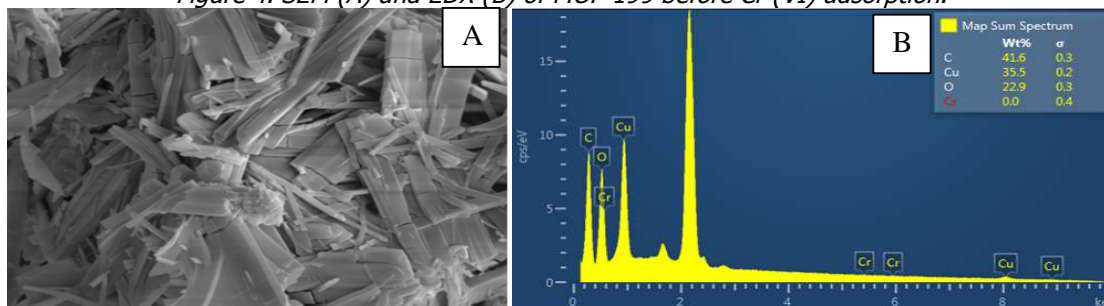


Figure 5 SEM (A) and EDX (B) of MOF-199 after Cr (VI) adsorption

Development of regression model analysis

Table 2 Design matrix for three variables together with the actual and predicted response

Std	Run	A:Conc. (mg/L)	B: Dosage (mg)	C:Time (Minutes)	Efficiency (%)	
					Actual Values	Predicted Values
11	1	30	63.6359	67.5	65.31	65.03
17	2	30	30	67.5	67.69	67.90
5	3	10	10	120	84.49	84.71
3	4	10	50	15	59.99	61.24
12	5	30	30	20.7941	59.92	58.88
4	6	50	50	15	61.15	60.87
6	7	50	10	120	66.99	65.68
18	8	30	30	67.5	67.66	67.90
10	9	30	3.63586	67.5	71.17	70.77
15	10	30	30	67.5	68.73	67.90
2	11	50	10	15	62.66	63.74
9	12	63.6359	30	67.5	59.23	59.74
8	13	50	50	120	61.97	61.92
19	14	30	30	67.5	67.02	67.90
13	15	30	30	155.794	75.38	76.92
14	16	30	30	67.5	67.86	67.90
1	17	10	10	15	64.33	64.31
7	18	10	50	120	81.91	80.76
16	19	30	30	67.5	68.54	67.90

As suggested by the central composite Design for percentage removal of Cr (VI) ions using MOF-199 adsorbent, the model was 2FI. Due to the higher order polynomial is reported in Table 2 and described in terms of the coded parameters by the second order polynomial equation as given in equations 2.

Table 3: Model summary statistics for percentage removal of Cr (VI) ions using MOF-199

Source	Std. Dev.	R ²	Adjusted R ²	Predicted R ²	PRESS	Comments
Linear	3.42	0.8036	0.7643	0.6059	352.30	
2FI	0.4576	0.9972	0.9958	0.9806	17.34	Suggested
Quadratic	0.4936	0.9975	0.9951	0.9717	25.26	
Cubic	0.2714	0.9996	0.9985		*	Aliased

$Cr(VI)Efficiency = 67.63 - 4.86 A - 1.49 B + 5.65 C + 0.3029 AB - 4.69 AC - 0.1450 BC$
 The above equations explain the relative impact of individual factors and interactive effects on Cr (VI) adsorption onto MOF-199 adsorbent. It can also be used to make predictions about the responses for any given levels of factors given. The analysis of variance corresponding to Equation 2 is reported in Table 4

Table 4: Analysis of variance (ANOVA) for percentage removal of Cr (VI) ions using MOF-199

Source	Sum of Squares	df	Mean Square	F-value	p-value	
Model	895.67	6	149.28	879.36	< 0.0001	significant
A-Conc.	252.69	1	252.69	1488.53	< 0.0001	
B-Dosage	30.48	1	30.48	179.52	< 0.0001	
C-Time	435.55	1	435.55	2565.74	< 0.0001	
AB	0.7338	1	0.7338	4.32	0.0597	
AC	176.05	1	176.05	1037.08	< 0.0001	
BC	0.1682	1	0.1682	0.9911	0.3391	
Residual	2.04	12	0.1698			
Lack of Fit	1.67	7	0.2384	3.24	0.1073	not significant
Pure Error	0.3684	5	0.0737			
Cor Total	897.70	18				

The Model F-value of 879.36 for Cr (VI) implies the model is significant. There is only a 0.01% chance that an F-value this large could occur due to noise in the case of Cr (VI). P-values less than 0.0500 indicated that the model terms are significant. In this case A, B, C, AC is significant model terms for Cr (VI). Values greater than 0.1000 indicated that the model terms are not significant. If there are many insignificant model terms (not counting those required to support hierarchy), model reduction may improve a model (Bayuo et al., 2020). The Lack of Fit F-value of 3.24 implied that the Lack of Fit is not significant relative to the pure error. There is a 10.73% chance that a Lack of Fit F-value this large could occur due to noise. Non-significant lack of fit is good as the model desired to fit. The low residual values obtained implied strong agreement between the experimental and predicted values. The values of R² and R²_{adj} were found to be 0.9977 and 0.9966 for percentage removal of Cr (VI) ions using MOF-199. This suggested that the process parameters analyzed explained about 99.78% for Cr (VI).

Isotherm, kinetics and thermodynamics studies

With the results obtained, adsorption isotherms were plotted to generate the Langmuir and

Freundlich data respectively (Table 5). It was found that, the Cr (VI) adsorption process fits a Langmuir adsorption mechanism, as the results produced a straight line with a reasonable regression value of 83.98%. The kinetics data was analyzed using the two most frequently used kinetic models, pseudo-first order and pseudo-second order. Correlation coefficient was found to be 0.40229, and the calculated q_e is not equal to experimental q_{eq} , suggesting the insufficiency of pseudo-first-order model to fit the kinetic data for the optimized Cr (VI) concentration examined. For the pseudo-second order kinetic model, correlation coefficient was found to be 0.99909 for optimized Cr (VI) concentration of 10 mg/L. the calculated q_e was found to be in agreement with the experimental q_{eq} . The rate constants and the correlation coefficients for both the tested models have been calculated and summarized in Table 6. Thermodynamic behavior of adsorption of Cr (VI) on MOF-199 was evaluated by the thermodynamic parameters and was studied at 298, 308 and 313 K as presented in Table 7. It was clear that the reaction showed spontaneity and endothermic nature of adsorption due to the negative values of ΔG^0 at all temperatures.

Table 5: Langmuir and Freundlich isotherm constants for Cr (VI) at room temperature

Langmuir Isotherms		Freudlich Isotherm	
K_L	1.293029	n	2.43415
R_L	0.071786	K_f	2.052134
R^2	0.83987	R^2	0.79888

Table 6: Pseudo-first Order and Pseudo-second Order Kinetic Models

	Pseudo 1st order	Pseudo 2nd order
q_e (exp.) (mg/g)	14.4336	14.4336
q_e (Cal.) (mg/g)	4.105633	15.37752
K_1 (min ⁻¹)	0.000227	0.03834
R^2	0.40229	0.99909

Table 7: Thermodynamic parameters for the adsorption of Cr (VI) using MOF-199

Temp.(K)	K_L	ΔG^0 (KJmol ⁻¹)	ΔH^0 (KJmol ⁻¹)	ΔS^0 (Jmol ⁻¹)
298	1.44336	-0.9092		
308	1.566677	-1.14965	-0.00091	34.05581
313	1.744955	-1.44876		

CONCLUSION

The present study revealed that MOF-199 was an effective adsorbent for the adsorption of Cr (VI) ions from aqueous solution. The optimization of Cr (VI) adsorption using MOF-199 was determined at an initial concentration of 10 mg/L, adsorbent dosage of 50 mg and contact time of 120 minutes. Under these optimized conditions, maximum Cr (VI)

adsorption was 84.771% with a desirability of 1.000. The process has the maximum efficiency at that operating condition. The adsorption isotherms could be well fitted by the Langmuir equation. The kinetics of the biosorption of Cr (VI) was better described with second-order kinetics. Gibbs free energy (ΔG^0) shows that adsorption processes studied are spontaneous.

REFERENCES

- Alfe, M., Gargiulo, V., Lisi, L. And Capua, R. (2014) Synthesis and characterization of conductive copper-based metal-organic framework/graphene-like composites. *Materials Chemistry and Physics* 147: 744-750.
- Bayuo, J., Abukari, M.A. and Pelig-Ba, K.B. (2020). Optimization using central composite design (CCD) of response surface methodology (RSM) for biosorption of hexavalent chromium from aqueous media. *Appl Water Sci* 10, 135.
- Chagas, P.M.B., Caetano, A.A., & Rossi, M.A., Gonçalves, M.A., Ramalho, T.C., & Corrêa, A.D. and Guimarães, I. R. (2019) Chitosan-iron oxide hybrid composite: mechanism of hexavalent chromium removal by central composite design and theoretical calculations. *Environmental Science and Pollution Research* (<https://doi.org/10.1007/s11356-019-04545-z>).
- Chui, S. S.-Y. Lo, S. M.-F. Charmant, J. P. H. Orpen, A. G. and Williams, I. D. (1999) A Chemically Functionalizable Nanoporous Material [Cu₃(TMA)₂(H₂O)₃]_n. *Science*, 283(5405), 1148-1150.
- Ghorbani-Kalhor, E. (2016) A metal-organic framework nanocomposite made from functionalized magnetite nanoparticles and HKUST-1 (MOF-199) for preconcentration of Cd(II), Pb(II), and Ni(II). *Microchim Acta* 183:2639-2647.
- Giraldo, L., Bastidas-Barranco, M., Húmpola, P. and Moreno-Piraján, J. (2017) Design, synthesis and characterization of MOF-199 and ZIF-8: Applications in the adsorption of phenols derivatives in aqueous solution. *European Journal of Chemistry* 8(3) 293-304.
- Lestari, W. W., Adreane, M., Purnawan, C., Fansuri, H., Widiastuti, N. and Rahardjo, S. B. (2016) Solvothermal and electrochemical synthetic method of HKUST-1 and its methane storage capacity. *Materials Science and Engineering* 107: 012030.
- Li, L., Liu, X. L., Geng, H. Y., Hu, B., Gong Wu Song, G., w and Xu, Z.S. (2013). A MOF/graphite oxide hybrid (MOF: HKUST-1) material for the adsorption of methylene blue from aqueous solution. *Journal of Materials Chemistry A*.

Special Conference Edition, April, 2022

- Liu, Z., Fan, A. and Ho, C. (2020) Preparation of AC/Cu-BTC Composite and Its Adsorption Mechanisms. *J. Environ. Eng., 146(4): 04020018.*
- Mahadi, N., Misran, H., Othman S. Z., Jamaludin, N. S. Manap, A. and Anuar, N. F. S (2015) Hydrothermal Synthesis and Characterizations of MOF-199 Using Renewable Template. *Applied Mechanics and Materials 773-774: 226-231.*
- Maleki, A., Hayati, B., Naghizadeh, M., Sang W. Joo, S. (2015) Adsorption of hexavalent chromium by metal organic frameworks from aqueous solution *Journal of Industrial and Engineering Chemistry: 211-216.*
- Petit, C and Bandosz, J. (2012) Exploring the coordination chemistry of MOF-graphite oxide composites and their applications as adsorbents. *Dalton Trans 41:4027-4035.*
- Petit, C., Burrell, J. and Bandosz, T. J. (2011). The synthesis and characterization of copper-based metal-organic frameworks/graphite oxide composite. *Carbon 49:563-572*
- Rodriguez, M., Rimoldi, F., Colombo, V., Sironi, A. and Carlucci, L. (2015) Metal-Organic Frameworks (MOFs)-Graphene Composites: Growth and Characterization of HKUST-1 on functionalized graphene layers for gas storage applications. *Graphita.*
- Sheno, N., Ali Morsali, A., and Joo, S. (2014) Synthesis CuO nanoparticles from a copper(II) metal-organic framework precursor *Materials Letters 117 (2014) 31-33.*
- Shi, R., Zhang, Z., Fan, H., Zhen, T. and Mi, J. (2017). Cu-based metal organic framework/activated carbon composites for sulfur compounds removal. *Applied Surface Science 394: 394-402.*
- Zhang, S., Du, Z. and Li, G. (2013). Metal-organic framework-199/graphite oxide hybrid composites coated solid-phase microextraction fibers coupled with gas Chromatography for determination for organochlorine pesticides from complicated samples. *Talanta 115: 32-39.*
- Zhao, Y., Cao, Y. and Zhong, Q. (2014) CO₂ Capture on Metal-Organic Framework and Graphene Oxide Composite Using a High-Pressure Static Adsorption Apparatus. *Journal of Clean Energy Technologies, Vol. 2(1)34-37*